In Silico Evaluation of Benzimidazole-Derived Heterocycles as CYP51-Targeting Antifungal Agent: Molecular Docking, Dynamics, and ADME Analysis

Mohammed Abdul Jabbar*, Ayad Kareem Khan*, Mohammed M. Al-Akaidi, Karima Fadhil Ali***

Department of Pharmaceutical Chemistry, College of Pharmacy, Mustansiriyah University, Baghdad-Iraq.

****Clinical Teaching Fellow, University of Leicester, UK.***

Article Info:

Received 25 Jan 2026
Revised 25 Apr 2026
Accepted 13 May 2026
Published 30 Jun 2026
Corresponding Author email:
mohammedabdaljabar@uomustansiriyah.edu.iq
Orcid: https://orcid.org/0009-0008-0273-6587

DOI: https://doi.org/10.32947/ajps.v26i2.1382

Abstract:

To counter the rising clinical threat of azole-resistant strains of Candida albicans, here, the design and computational validation of new benzimidazole-based heterocycles designed to inhibit the enzyme CYP51 is investigated. Employing a combination of GOLD-dependent molecular docking and 200-nanosecond-long Desmond molecular dynamics simulations, we were able to identify lead candidates, i.e., compounds with bulky substituents, with significantly higher binding affinity when compared to the clinical reference, fluconazole, exploiting deep hydrophobic sub-pockets in the active site. The observed structural stability of the MD trajectories, together with a lack of Lipinski rule violations in the ADMET profiling using QikProp, indicates that these derivatives have the necessary drug likeness for efficacious oral delivery. Ultimately, the synergy between high-occupancy lipophilic anchors and favorable pharmacokinetic parameters positions these heterocyclic scaffolds as high-priority candidates for synthetic expansion and subsequent *in vitro* antifungal screening. Nonetheless, since these results are purely predictive and constrained by the in-silico character, synthetic expansion and in turn in vitro and in vivo validations must be carried out to establish their clinical efficacy and safety.

Keywords: Benzimidazole derivatives, Antifungal agents; CYP51 inhibitors; Molecular docking; Molecular dynamics; ADMET prediction.

التقييم الحاسوبي للمركبات الحلقية غير المتجانسة المشتقة من البنزيميدازول كعوامل مضادة للفطريات تستهدف إنزيم CYP51: دراسة الإرساء الجزيئي، الديناميكا الجزيئية، وتحليل الخصائص الدوائية (ADME)

محمد عبد الجبار*، أياد كريم خان*, محمد م. العكيدي **، كريمة فاضل علي*

***قسم الكيمياء الصيدلانية، كلية الصيدلة، جامعة المستنصرية، بغداد-العراق.*

****زميل تدريس سريري، جامعة ليستر، المملكة المتحدة.***

AJPS is licensed under a Creative Commons Attribution 4.0 International License

الخلاصة:
لمواجهة التحدي السريري المتزايد المتمثل في مقاومة فطر المبيضات البيضاء (Candida albicans) لمجموعة الأزول، تستقصي هذه الدراسة تصميم وتحققاً حاسوبياً لمركبات حلقية غير متجانسة جديدة مشتقة من البنزيميدازول تستهدف إنزيم CYP51. ومن خلال الجمع بين تقنية الإرساء الجزيئي المستندة إلى برنامج (GOLD) ومحاكاة الديناميكا الجزيئية عبر برنامج (Desmond) لمدة 200 نانو ثانية، تمكنا من تحديد عدد من المركبات الرائدة، لا سيما تلك التي تحتوي على مجموعات مستبدلة ضخمة؛ حيث أظهرت هذه المركبات ألفة ارتباط أعلى بكثير مقارنة بالمرجع السريري فلوكونازول، وذلك من خلال استغلال الجيوب الفرعية العميقة الكارهة للماء داخل الموقع النشط للإنزيم.
وقد أظهرت نتائج مسارات الديناميكا الجزيئية استقراراً بنيوياً ملحوظاً، ترافق مع خلوّ تام من أي مخالفات لقواعد ليبينسكي وفقاً لتوصيف الخصائص الدوائية ببرنامج (QikProp). مما يشير إلى أن هذه المشتقات تمتلك الخواص الدوائية اللازمة للإعطاء الفعال عن طريق الفم. وفي الختام، فإن التآزر بين المرتكزات المحبة للدهون عالية الإشغال والمعايير الحركية الدوائية المواتية، يجعل من هذه الهياكل الحلقية مرشحات ذات أولوية عالية للتوسع في التخليق الكيميائي وإجراء الفحوصات المخبرية اللاحقة لمضادات الفطريات

الكلمات المفتاحية: مشتقات البنزيميدازول؛ عوامل مضادة للفطريات؛ مثبطات CYP51؛ الإرساء الجزيئي؛ الديناميكا الجزيئية؛ التنبؤ بخصائص ADMET.

Introduction

Invasive fungal infection has become a growing threat with high morbidity and mortality due to the widespread use of glucocorticoids, broad-spectrum antimicrobials, and AIDS chemotherapy drugs, as well as the use of invasive procedures such as hemodialysis, deep vein catheterization, and transplantation. Modern estimates show that 1.5 -2 million people die of fungal diseases every year (1–3). To address this health issue of concern, the World Health Organization (WHO) in 2020 established the Advisory Group on the Fungal Priority Pathogens List (AG -FPPL). The group published the first Fungal Priority Pathogens List (FPPL) in 2022, aimed at guiding global research, development, and public health actions to address fungal infections and their associated drug resistance issues (4).

The clinical manifestation of Candida albicans is significantly complex, which predetermines its inclusion in the Fungal Priority Pathogens List (FPPL) as a high-priority organism. Even though it is most commonly found as an innocent ingredient of the human microbiome, it has an alarming tendency to develop into a major pathogen in case of host immune defenses being weakened (5). It has a widespread clinical footprint, which is evident in the form of well-reported mucosal infestations, including neonatal oral thrush and vulvovaginal candidiasis (6).

One of the major issues for clinicians, however, is its ability to trigger invasive disease. When the organism has invaded the blood, the ability of the organism to cause extensive tissue destruction may take place, as it can attack other sensitive organs such as the heart, brain, and other crucial structures (7).

This systemic transition is a life-threatening complication with a sobering mortality rate. Although there are therapeutic interventions in place, the complication is still marked by a high mortality rate of up to 30 percent, especially among immunocompromised patients (8).

Benzimidazoles are annular privileged heterocyclic structures with a wide array of biological and pharmaceutical properties. Synthetic chemists have extensively explored benzimidazole scaffolds over the years, making them one of the most studied compound classes (9–13). Azole-resistant C. albicans infections commonly show

AJPS is licensed under a Creative Commons Attribution 4.0 International License

resistance to traditional antifungal therapies. Candida albicans becomes resistant to azoles by overproducing efflux pumps within the cell. These pumps are transporters associated with the membrane that confer resistance by preventing the intracellular accumulation of drugs, which in turn prevents toxic levels that would lead to cell death (14,15). This overexpression of efflux pumps often confers cross-resistance between azoles in vitro and clinically in C. albicans (16). Upregulation of the efflux pump-related genes *CDR1* and *CDR2* is mainly responsible for the resistance of *C. albicans* (17). Future research should concentrate on discovering and validating novel antifungal compounds to combat this global health threat.

As an enzyme, 14a-demethylase (CYP51) is a structurally characterized and well-validated antifungal target (Fig. 1) that has resulted in the approval of various azole drugs as CYP51 inhibitors by the FDA, including fluconazole and itraconazole (18,19). The CYP51 inhibitors have their antifungal effect by disrupting ergosterol, a crucial constituent of fungal cell membranes, biosynthesis. The heme in CYP51 is bound by the triazole moiety, which is specific to the structure of azole drugs. Nevertheless, over the past years, reports of ever-growing drug resistance have arisen, which demonstrates the possibility of resistance to this type of drug. Antifungal agents that have new scaffolds require urgent development (20–22).

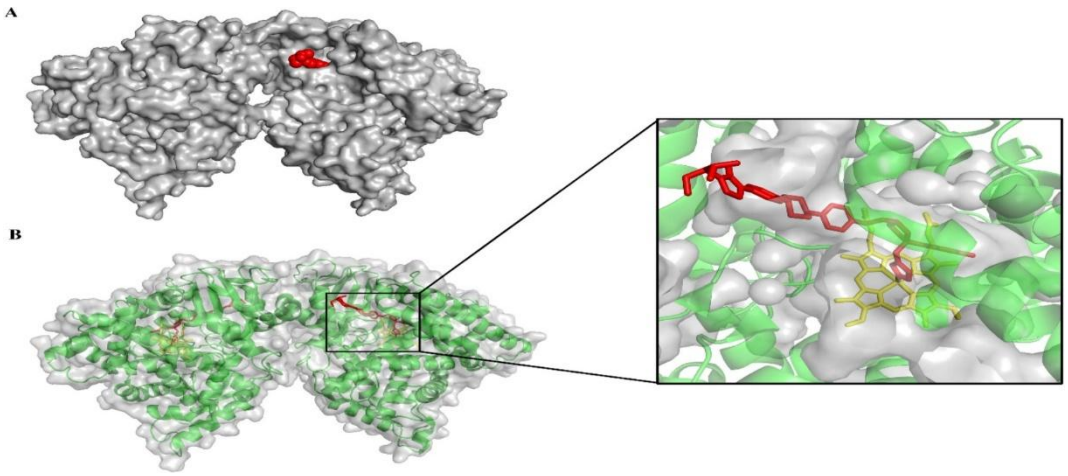

Figure 1: Modelled binding modes and three-dimensional interaction topologies of the benzimidazole derivatives in the active site of CYP51 (PDB ID: 5FSA).

Panel (A) shows the orientation of the lead candidate with respect to the heme cofactor, and the distance between the coordination points in Angstroms (Å). The interaction map in detail in Panel (B) uses colored lines: pink dashed lines indicate hydrogen bonds, and green lines indicate hydrophobic interactions. Hydrophobicity (blue hydrophilic, brown lipophilic) coloring of the receptor surface is used to indicate the use of the deep hydrophobic sub-pockets.

Accordingly, the present study aims to design and evaluate new benzimidazole-derived heterocyclic compounds as potential CYP51 inhibitors using an integrated in silico approach, including molecular docking, molecular dynamics simulations, and ADMET profiling, to identify promising candidates for further experimental validation.

AJPS is licensed under a Creative Commons Attribution 4.0 International License

2. Materials and methods

Ligands Preparation

The choice of the six benzimidazole-based ligands (1–6) was guided, strategically, by the desired Structure-Activity Relationship (SAR) rationale, directed towards investigating the topographical and electronic specifications of the CYP51 active site. Compound 1, with a hydrogen atom at the R-position, was chosen as the structural template of the series. The R-group was then substituted with substituents of different electronic and steric profiles to chart the preferences of the binding pocket in a systematic manner. Particularly, the methyl (–CH 3) and methoxy (–OCH 3) groups were added to evaluate the effects of small to moderate steric bulk and electron-donating effects. To give the molecules a higher bulk and basicity, a dimethylamino (–N(CH 3) 2 group was chosen, and a nitro (–NO 2) group was used to test how the enzyme would respond to a strong electron-withdrawing group. Lastly, a phenyl ring was added to explore the effect of longer aromaticity and large lipophilic volume. This controlled deviation permits the full assessment of the forces acting to dictate optimal binding affinity, and the utilization of the deep hydrophobic sub-pockets present in the enzyme.

The stable conformation of the ligands shown in Figure 2 was achieved by initially sketching the suggested compounds in 2D using ChemDraw version 23.1.1.3. Subsequently, these compounds were converted into 3D representations utilizing Chem3D version 23.1.1.3. The MM2 force field was used for energy minimization (23).

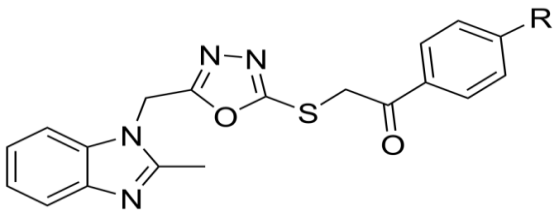

Compound No.	R Group
1	H
2	CH_3
3	OCH_3
4	$N(CH_3)_2$
5	NO_2
6	Phenyl

Figure 2. Structures of the designed compounds

Molecular Docking procedure

The full-license version of Genetic Optimization for Ligand Docking (GOLD) (v. 5.6.2) was used for molecular docking to investigate the full range of ligand conformational flexibility alongside protein partial flexibility (24). The Hermes visualizer program in the GOLD Suite was used to configure the receptors for the docking process. The binding location for GOLD docking was defined as all protein residues within 10 A° of reference ligands in the downloaded protein structure complexes (25). The 5FSA protein was acquired from the PDB database for the ligand docking investigation. The protein's cavity and active site were determined using a reference ligand with an active site radius of 10 A°. Set the

AJPS is licensed under a Creative Commons Attribution 4.0 International License

Piecewise Linear Potential (PLP) as the appropriate scoring function. Analyzing the docking results by looking at hydrogen bonds, brief contacts, bond length, and other vital interactions to determine the protein-ligand binding poses and interactions.

2.1. Validation of docking feasibility

To assess the accuracy and reproducibility of the docking procedure, a systematic validation protocol involving redocking and structural superimposition was employed. To validate the docking accuracy for CYP51 (PDB ID: 5FSA; resolution: 2.86 Å), the reference drug fluconazole was redocked into the defined active site using the same docking parameters as in the initial docking (26).

2.2. Protein preparation and molecular docking simulation

The 3D structure of the target enzyme, lanosterol 14a-demethylase (PDB ID: 5FSA; resolution: 2.86 A), was obtained at the Protein Data Bank. The protein underwent a stringent preparation procedure to guarantee a high-fidelity docking environment. This procedure included assigning the correct bond orders systematically, adding the missing hydrogen atoms, and eliminating all the crystallographic water molecules and heteroatoms located more than 10 Å away from the active site. The hydrogen-bond network was further optimized to a physiological pH of 7.4 to perfectly show the ionization states of the amino acid residues. The endogenous heme cofactor was given special consideration and was retained and parameterized accordingly to maintain its essential contribution to the architecture of the active site and possible coordination with the benzimidazole ligands.

Molecular dynamics simulation

With the Desmond modules of Schrodinger 2024, Molecular Dynamics was performed on the derivative with the best docking score (28). The OPLS4 force field was utilized to model protein interactions, and it was noted for its accuracy and comprehensive coverage of chemical space relevant to drug discovery. The purpose of defining the simulation box is to reduce the solvent volume while ensuring adequate solvent presence around the solute, thereby preventing the protein from detecting a periodic image of itself during the simulation. Sodium ions were injected to set up a charge-neutral milieu for the protein-ligand complex, and 0.15 M of sodium chloride (NaCl) was included to imitate the natural system. The system was built using the TIP3P solvent model. The simulation lasted 200 ns. The NPT ensemble class was active, with the system energy set to 1.2. The simulation was configured to run at 1.01325 bar and 300 K. The simulation interaction diagram was developed after examining the relaxed simulated system (29).

ADMET prediction

To assess the pharmacokinetic and drug-likeness of the developed benzimidazole derivatives, we used QikProp module (Schrodinger Suite). The choice of ADMET assessment criteria, shown in Table 2, was based on the need to ensure high oral bioavailability and systemic stability, which are important for treating invasive candidiasis.

First, the Lipinski Rule of Five (Molecular Weight < 500 Da, octanol/water partition coefficient [Log P] < 5, Hydrogen Bond Donors < 5, Acceptors < 10) was considered to narrow down candidates with good passive membrane permeability and intestinal absorption. In order to further improve these predictions, the Topological Polar Surface Area (TPSA) was computed since it is a powerful predictor of a molecule's capacity to penetrate cellular membranes. Since systemic C. albicans infections may cross the blood-brain barrier, resulting in fungal meningitis, we also measured CNS activity and Brain/Blood partition coefficients (Log BB). The parameters are important to decide

AJPS is licensed under a Creative Commons Attribution 4.0 International License

whether the compounds are able to penetrate deep-seated infections in the central nervous system. Lastly, the Human Oral Absorption (HOA) percentages were forecasted to support the effectiveness of these scaffolds in delivering drugs orally, avoiding the need to do it intravenously (30–32).

Results and Discussion

In-silico studies are crucial to the drug development process, serving as a powerful instrument for forecasting the therapeutic efficacy of novel medications. They also aid in reducing the time and resources needed for the process, and when employed in conjunction with other strategies, they increase the likelihood of producing effective medications. We used rigorous and proven computational modules to validate the results.

Molecular Docking results

The antifungal agent fluconazole and the target protein 5FSA have been investigated with six proposed compounds. The results are presented in Table 1, which details the predicted mean PLP fitness, hydrogen bonds, and hydrophobic interactions for both the compounds under study and the reference ligands. The prevalence of short contacts in each substance exceeded that of hydrogen bonding. The predominance of hydrophobic interactions over hydrogen bonding contacts, which are essential for substrate binding to an active site, suggests that pharmacological activity is enhanced with an increase in the number of hydrophobic contacts (33). The results predict that the compounds under study demonstrate greater efficacy as antifungal agents than fluconazole, with the same interaction patterns within the active site of the targeted receptor.

Table 1: The fitness score of proposed ligands and the reference drug

Compound	PLP Fitness	H-bonds	Short contacts
Compound 4 $N(CH_3)_2$	106.9	TYR118, TYR132, HEM580,	TYR64, PRO230, GLY307, THR311, LEU376, MET508.
Compound 6 (Phenyl)	106.4	TYR118, TYR132, HEM580,	PRO230, GLY307, PHE380, MET508.
Compound 5 (NO_2)	105.3	TYR118, TYR132, HEM580,	TYR64, THR311, LEU376, MET508.
Compound 2 (CH_3)	101	TYR118, TYR132, HEM580,	TYR118, PRO230, GLY307, LEU376,
Compound 3 (OCH_3)	101	TYR118, TYR132, HEM580,	TYR118, LEU121, PRO230, GLY307, THR311.
Compound 1 (H)	98.7	TYR118, TYR132, HEM580.	TYR132, GLY307, LEU376, MET508.
Fluconazole	76.4	TYR132, HEM580.	TYR118, LEU376.

The Structure-Activity Relationship (SAR) of the synthesized benzimidazole series indicates a clear dependence between the physicochemical characteristics of the R-substituent and the observed activity against CYP51. All derivatives showed positive binding, but with high affinity achieved with the phenyl (Compound 6) and dimethylamino (Compound 4) substituted analogs, giving important mechanistic information.

These bulky, lipophilic groups cannot be attributed to simply occupying space, but the superior performance of the bulky groups can be attributed to the replacement of the ordered water molecules inside the deep hydrophobic sub-pockets of the enzyme.

AJPS is licensed under a Creative Commons Attribution 4.0 International License

These lipophilic cavities are frequently filled in the unbound form of the protein by highly ordered, energetically dissatisfied water molecules, which are unable to form a complete set of hydrogen bonds. The entry of big, hydrophobic moieties has the effect of pushing out these water molecules into the bulk solvent. The consequence of this transition is a huge rise in the solvent entropy and a strong entropically driven thermodynamic force that stabilizes the protein-ligand complex.

Moreover, the surface area of the CYP51 pocket is optimized by the close spatial complementarity of these bulky R-groups with the aromatic residues that line the pocket. The latter is supported by the fact that these complexes are more stable in the 200 ns MD trajectories. Conversely, the fact that the nitro-substituted analogue (Compound 5) is relatively less fit indicates that the energetic cost of desolvating a highly polar functional group to access a hydrophobic cleft is a stronger factor than the potential of polar contacts in this part of the CYP51 active site.

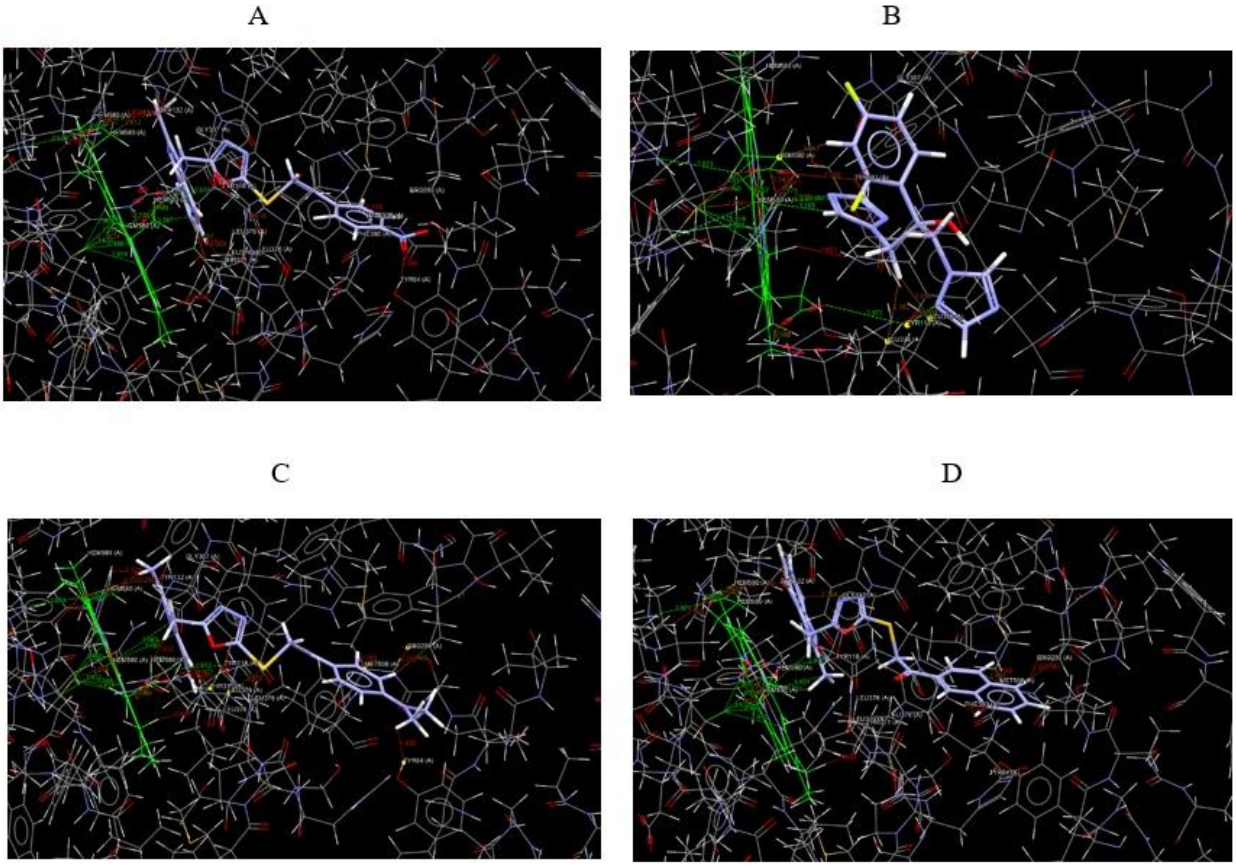

Figure 3: The compounds–protein complex structure (A: Compound 4, B: Compound 6, C: Compound 5, D: Fluconazole).

Molecular dynamics simulation (MDS)

An MDS analysis was performed on the compound 4-5FSA complex, enabling investigation of the dynamic behavior of the protein-ligand complex. Molecular dynamics (MD) simulation has proven to be an efficient tool for exploring conformational space and is often used to analyze macromolecular ligand-receptor interactions.

AJPS is licensed under a Creative Commons Attribution 4.0 International License

Furthermore, MD modeling excels in accommodating proteins' mobility and flexibility. To assess the stability of the protein-ligand complex, MD simulations were performed on the top-scoring ligand to track its conformational changes and interaction consistency throughout the simulation trajectory. The dynamic behavior of ligand 4-5FSA was monitored and recorded for 200 ns. The stability of the initial 40 ns, as indicated by the sharp rise in the red trace.

The ligand RMSD plateau at a ligand conformation of 5.2Å indicates that the ligand has changed its original docked position to a more energetically stable binding pose in the pocket. The fact that both protein and ligand RMSD curves converged near the end stage of the simulation shows that the system is at dynamic equilibrium, thus creating a solid point to base future thermodynamic analyses.

protein-ligand complex was examined using the RMSD and RMSF measurements. Figure 4 shows the root-mean-square deviation (RMSD) trajectory of the protein-ligand complex simulated within 200ns. The protein backbone is shown to be very stable with an RMSD of between 1.6 and 2.4 Å, and the ligand undergoes a large conformational change in the

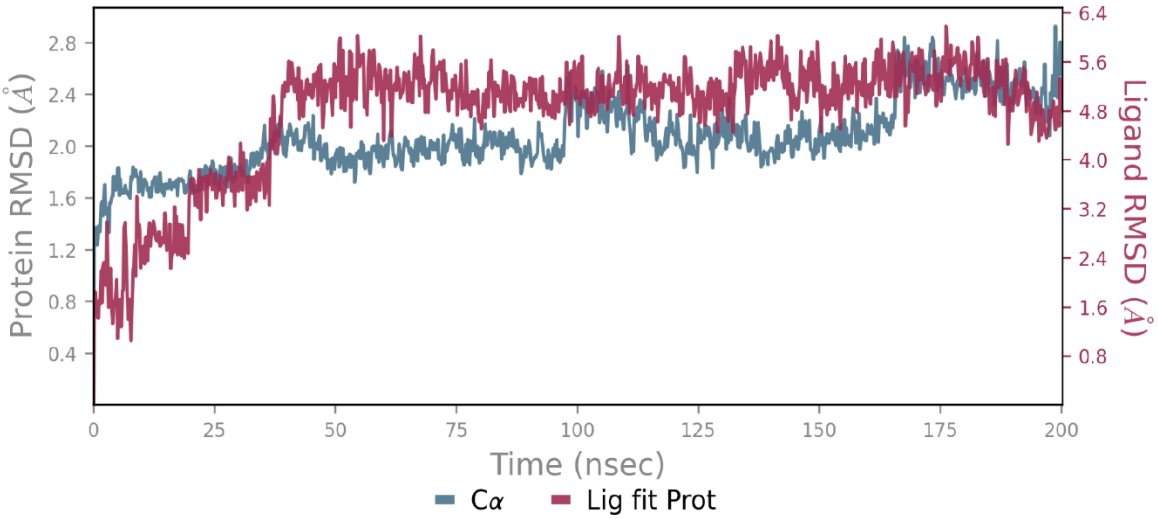

Figure 4: Compound 4 – Protein Complex RMSD

Figure 5 shows that the root-mean-square fluctuation (RMSF) profile of the protein shows an overall inflexible architecture, with areas of high flexibility appearing in local regions, especially around the 380-410 residue location. The RMSF values of residues in general are below 1.5 Å, and the high peaks are the residues of intrinsically

AJPS is licensed under a Creative Commons Attribution 4.0 International License

disordered or highly dynamic loops, which probably increase the solvent accessibility. The green labels point to residues whose fluctuations are minimal, and this means that the core binding pocket and functional motifs are similarly conserved in structure to maintain the very specific geometry to recognize the ligand. This juxtaposition between single-minded functional units and a loose scaffold of the entire world underscores the fact that the protein is capable of preserving the structural integrity of the protein while allowing the required adaptive motions.

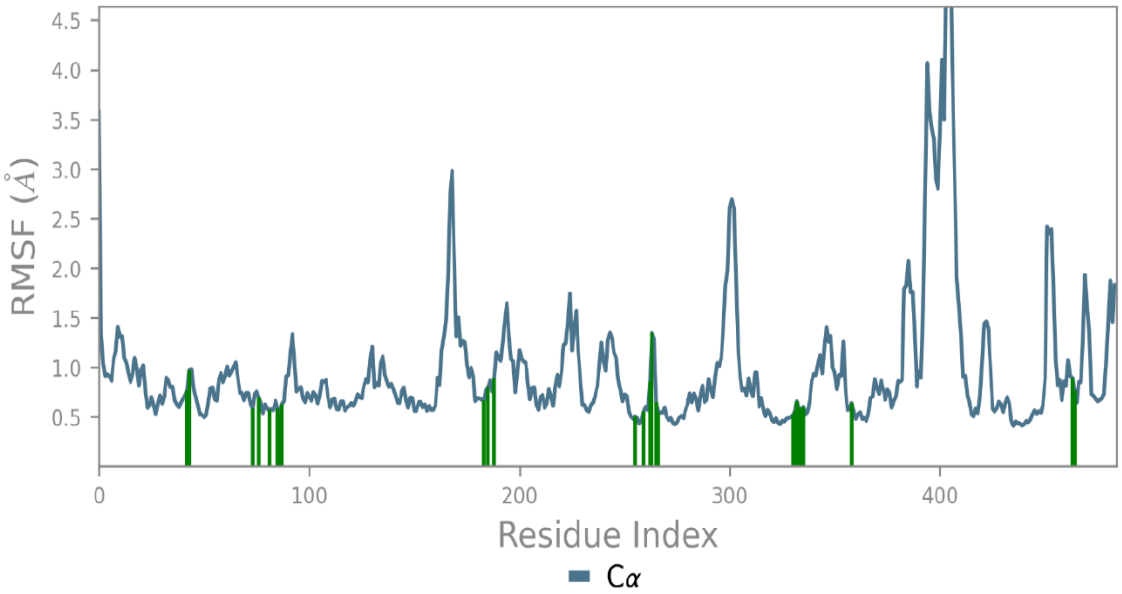

Figure 5: Root Mean Square Fluctuations (RMSF) of residue index.

According to the RMSF analysis, there are particular residues (marked in green) that are directly interacting with the ligand and exhibit significantly less fluctuations in their form, which confirms the presence of a rigid binding interface. On the contrary, the large peaks at the positions of residues 400 and above are associated with intrinsically flexible loops, which do not have a negative impact on the structural integrity of the active site. In the case of the ligand, the small RMSFs of Figure 6 of the heterocyclic core (atoms 1-13) as compared to the distal tail (atoms 16-29) support the stability of the principal docking points. The coincidental stability of both protein contact residues and ligand anchor positions is equal evidence of a high-affinity binding event with insignificant structural strain.

AJPS is licensed under a Creative Commons Attribution 4.0 International License

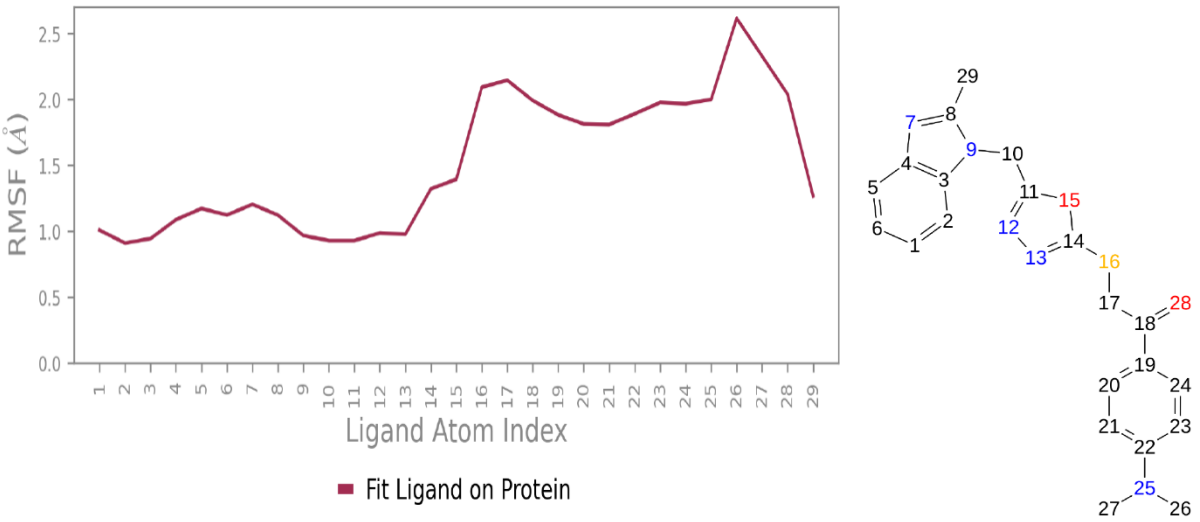

Figure 6: The Ligand Root Mean Square Fluctuation (L-RMSF)

A closer look at the binding site shown in Figure 7 shows that a high-density hydrophobic network around PHE126 and ILE131 is the major stabilizing factor of the complex, not polar interactions. These residues act as vital lipophilic anchors that facilitate ligand binding through a desolvation-based mechanism, which in effect packages the aromatic core out of the aqueous phase. The thermodynamic stability is higher with non-polar contacts than with transient bridges of water because the increased van der Waals packing has tight shape complementarity. The hydrophobic effect, therefore, limits the translational movement of the ligand, entrapping it firmly inside the interior of the protein during the simulation.

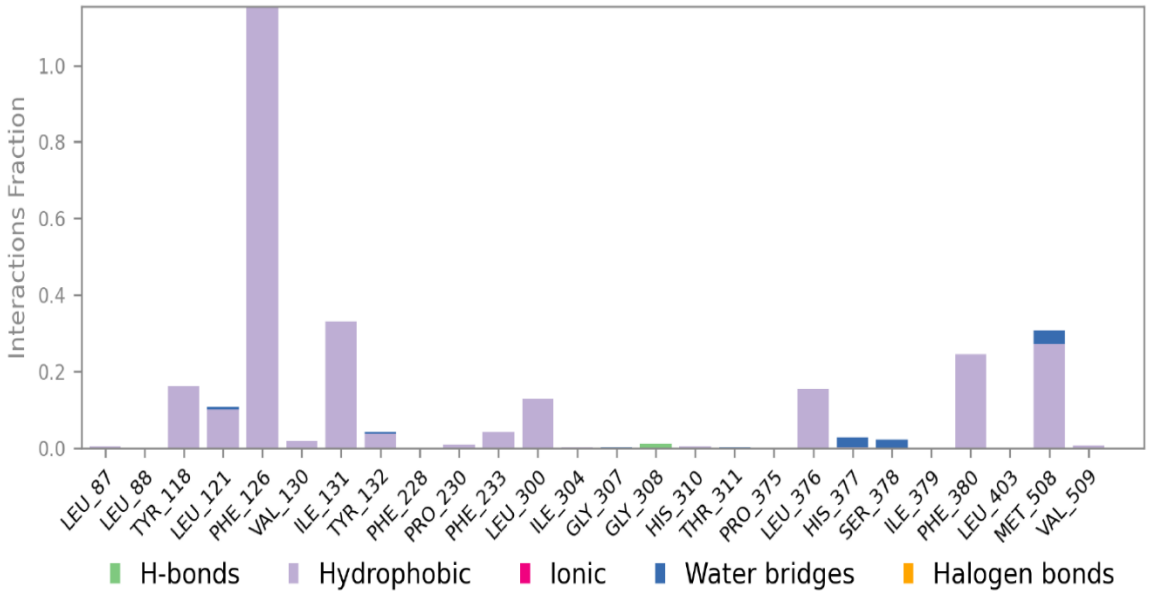

Figure 7: Protein-Ligand Contacts

AJPS is licensed under a Creative Commons Attribution 4.0 International License

ADME Study

Although the ADMET profiles obtained through QikProp could be used as a solid initial screen to determine whether the benzimidazole derivatives are drug-like, it must be noted that in silico pharmacokinetic modeling is imperfect in nature. Such computational predictions are essentially theoretical and are an idealistic estimate of a molecular behavior. In particular, in silico models are not able to accommodate the high complexity of human physiological pathways (i.e., the fine-tuning of Phase I and Phase II metabolic biotransformation or the impact of the gut microbiome on drug stability).

Moreover, whereas passive membrane permeability is predicted by our models, they might not completely describe active transport processes, including the affinity of these compounds to P-glycoprotein (P-gp) or other ABC transporters- a crucial factor in determining real systemic concentration and tissue distribution. Also, unpredictable in vivo toxicological events, such as idiosyncratic drug-induced organ damage or complicated immune-mediated effects, are out of the capabilities of current predictive algorithms. The current data on ADMET is, therefore, to be understood as a high-confidence prioritization tool to inform future research directions, but not as an absolute alternative to experimental in vivo and in vitro pharmacokinetic validation.

Table 2. The ADME study results of the proposed ligand and reference drug.

Molecule	Fluconazole	H	CH_3	Phenyl	$N(CH_3)_2$	OCH_3	NO_2	Normal Value
mol_MW	306.274	364.421	378.448	414.481	407.489	394.447	409.42	130.0 – 725.0
Donor HB	1	0	0	0	0	0	0	0.0 – 6.0
Accept HB	6.75	6	6	6	7	6.75	7	2.0 – 20.0
Water solubility	Soluble	Moderately soluble	Moderately soluble	Moderately soluble	Moderately soluble	Moderately soluble	Moderately soluble	
G.I Absorption	High	High	High	High	High	High	Low	>80% is high <25% is poor
TPSA	81.65	99.11	99.11	99.11	102.35	108.34	144.93	> 140 Å
BBB Permeability	No	No	No	No	No	No	No	
Rule Of Five	0	0	0	0	0	0	0	maximum is 4

Conclusion

Here, we used a combined computational approach in the design and screening of a series of benzimidazole-based heterocycles as new CYP51 enzyme inhibitors in the fungus. We show that the strategic addition of bulky, lipophilic groups - the dimethylamino and phenyl groups in Compounds 4 and 6 - greatly increases binding affinity, by taking advantage of

AJPS is licensed under a Creative Commons Attribution 4.0 International License

previously unexploited deep hydrophobic sub-pockets in the active site. These candidates, in addition to being superior to the clinical standard, fluconazole, in docking fitness, exhibited remarkable structural stability during demanding 200 ns molecular dynamics simulations.

Although these results are encouraging, we recognize that this research has limitations, such as being strictly in silico. Although our ADMET and MD simulations offer high-confidence predictions, they do not take into account the complexity of the physiological environment of living organisms, nor do they consider the possibility of unpredicted metabolic problems.

In turn, the work can be considered a roadmap to the next-generation antifungal development. The direct future actions of this project are the chemical synthesis of Lead Compounds 4 and 6 and the detailed in vitro minimum inhibitory concentration (MIC) studies of a series of azole-resistant Candida albicans strains. With this gap between computational design and experimental validation, we hope to validate these heterocyclic scaffolds as potential viable candidates to counter this growing global menace of antifungal resistance.

References:

1- Li X, Zhang H, Zhang J, Li Y, Wang H, Zhao W, et al. Design, synthesis and biological evaluation of 5-substituted sulfonylureas as novel antifungal agents targeting acetohydroxyacid synthase. J Mol Struct. 2022 Jul 5;1259:132714. doi: 10.1016/j.molstruc.2022.132714.

2- Jabli S, Hrichi S, Chaabane-Banaoues R, Molton F, Loiseau F, Roisnel T, et al. Study on the synthesis, physicochemical, electrochemical properties, molecular structure and antifungal activities of the 4-pyrrolidinopyridine Mg(II) meso-tetratolylporphyrin complex. J Mol Struct. 2022 Aug 5; 1261:132882.

3- Waseem M, Thakur J, Subbarao N. Prediction of novel and potent inhibitors of lanosterol 14-α demethylase. J Biomol Struct Dyn. 2022;41(11):5119-31. doi: 10.1080/07391102.2022.2096116.

4- Casalini G, Giacomelli A, Antinori S. The WHO fungal priority pathogens list: a crucial reappraisal to review the prioritisation. Lancet Microbe. 2024 Jul;5(7):717-24. doi: 10.1016/S2666-5247(24)00042-9.

5- Parambath S, Dao A, Kim HY, Zawahir S, Alastruey-Izquierdo A, Tacconelli E, et al. Candida albicans—A systematic review to inform the World Health Organization Fungal Priority Pathogens List. Med Mycol. 2024 Jun 27;62(6):myae045. doi: 10.1093/mmy/myae045.

6- Talapko J, Juzbašić M, Matijević T, Pustijanac E, Bekić S, Kotris I, et al. Candida albicans—The Virulence Factors and Clinical Manifestations of Infection. J Fungi (Basel). 2021 Jan 22;7(2):79.

7- Talapko, J.; Juzbašić, M.; Matijević, T.; Pustijanac, E.; Bekić, S.; Kotris, I.; Škrlec, I. Candida albicans—The Virulence Factors and Clinical Manifestations of Infection. J. Fungi 2021, 7, 79. https://doi.org/10.3390/jof7020079.

8- Tan E, Suryana K. Oral candidiasis and the risk factors: a serial case reports. Int J Adv Med. 2021 Sep;8(9):1415-9. doi: 10.18203/2349-3933.ijam20213247.

9- Chung NT, Dung VC, Duc DX. Recent achievements in the synthesis of benzimidazole derivatives. RSC Adv. 2023 Oct 31;13(46):32734-71.

10- Racané L, Zlatar I, Perin N, Cindrić M, Radovanović V, Banjanac M, et al. Biological Activity of Newly Synthesized Benzimidazole and Benzothizole 2,5-Disubstituted Furane Derivatives.

AJPS is licensed under a Creative Commons Attribution 4.0 International License

Molecules. 2021 Aug 13;26(16):4935. doi: 10.3390/molecules26164935.
11- Gaba M, Singh S, Mohan C. Benzimidazole: An emerging scaffold for analgesic and anti-inflammatory agents. Eur J Med Chem. 2014 Apr 9; 76:494-505.
12- Mulugeta E, Samuel Y. Synthesis of Benzimidazole-Sulfonyl Derivatives and Their Biological Activities. Biochem Res Int. 2022; 2022:7255299. doi: 10.1155/2022/7255299.
13- Adnan AMA, Mahdi MF, Khan AK. Design, synthesis, and acute anti-inflammatory assessment of new 2-methyl benzoimidazole derivatives having 4-thiazolidinone nucleus. Al Mustansiriyah J Pharm Sci. 2019;19(4):111-25.
14- Khan MI, Choudhry H, Jahan S, Rather IA. Reversal of Azole Resistance in Candida albicans by Human Neutrophil Peptide. Biomedicines. 2023 Feb 10;11(2):513. doi: 10.3390/biomedicines11020513.
15- Ceballos-Garzon A, Peñuela A, Valderrama-Beltrán S, Vargas-Casanova Y, Ariza B, Parra-Giraldo CM. Emergence and circulation of azole-resistant C. albicans, C. auris and C. parapsilosis bloodstream isolates carrying Y132F, K143R or T220L Erg11p substitutions in Colombia. Front Cell Infect Microbiol. 2023; 13:1136217. doi: 10.3389/fcimb.2023.1136217.
16- Pristov KE, Ghannoum MA. Resistance of Candida to azoles and echinocandins worldwide. Clin Microbiol Infect. 2019 Jul;25(7):792-8. doi: 10.1016/j.cmi.2019.03.028.
17- Zhang MR, Zhao F, Wang S, Lv S, Mou Y, Yao CL, et al. Molecular mechanism of azoles resistant Candida albicans in a patient with chronic mucocutaneous candidiasis. BMC Infect Dis. 2020 Feb 11;20(1):126. doi: 10.1186/s12879-020-4856-8.
18- Winston DJ, Maziarz RT, Chandrasekar PH, Lazarus HM, Goldman M, Blumer JL, et al. Intravenous and oral itraconazole versus intravenous and oral fluconazole for long-term antifungal prophylaxis in allogeneic hematopoietic stem-cell transplant recipients. A multicenter, randomized trial. Ann Intern Med. 2003 May 6;138(9):705-13. doi: 10.7326/0003-4819-138-9-200305060-00006.
19- Galgiani JN. Fluconazole, a new antifungal agent. Ann Intern Med. 1990 Aug 1;113(3):177-9. doi: 10.7326/0003-4819-113-3-177.
20- Zhang J, Li L, Lv Q, Yan L, Wang Y, Jiang Y. The Fungal CYP51s: Their Functions, Structures, Related Drug Resistance, and Inhibitors. Front Microbiol. 2019 Apr 24; 10:691.
21- Teixeira MM, Carvalho DT, Sousa E, Pinto E. New antifungal agents with azole moieties. Pharmaceuticals. 2022;15(11):1427. doi: 10.3390/ph15111427.
22- Yan Z, Huang Y, Zhao D, Li Z, Wang X, Guo M, Wei Y, Wang Y, Mou Y, Hou Z, Guo C. Developing novel coumarin-containing azoles antifungal agents by the scaffold merging strategy for treating azole-resistant candidiasis. J Med Chem. 2023;66(18):13247-13265. doi: 10.1021/acs.jmedchem.3c01254.
23- Mahmood SA, Mahdi MF, Rauf AMR, Aburjai T. In silico Study of New Five-Membered Heterocyclic Derivatives Bearing (1,3,4-oxadiazole and 1,3,4-thiadiazole) As Promising Cyclooxygenase Inhibitors. Al Mustansiriyah J Pharm Sci. 2024 Jul 9;24(3):237-51.
24- Jones G, Willett P, Glen RC, Leach AR, Taylor R. Development and validation of a genetic algorithm for flexible docking. J Mol Biol. 1997 Apr 4;267(3):727-48.
25- Alsalamy Z, Khan AK, Hamdi MD, Mehde AA. Drug Design, In Silico-Profiling of New Pyrrole Derivatives: Promising Anticancer Agents Against Acute Myeloid Leukemia. Al

AJPS is licensed under a Creative Commons Attribution 4.0 International License

Mustansiriyah J Pharm Sci. 2024 Jul 9;24(3):252-63.
26- Ahmad I, Khalid H, Perveen A, Shehroz M, Nishan U, Rahman FU, et al. Identification of Novel Quinolone and Quinazoline Alkaloids as Phosphodiesterase 10A Inhibitors for Parkinson's Disease through a Computational Approach. ACS Omega. 2024 Mar 26;9(14):16262-78. doi: 10.1021/acsomega.3c10351.
27- Abdull MT, Mahdi MF, Khan AK. Molecular docking, Synthesis and Characterization of New Indomethacin and Mefenamic Acid Analogues as Potential Anti-inflammatory Agents. Al Mustansiriyah J Pharm Sci. 2023 Jul 20;23(3):336-44.
28- Schrödinger Release Notes - Release 2024-3.
29- Shah A, Choudhary A, Jain M, et al. Discovery of novel anticancer flavonoids as potential HDAC2 inhibitors: virtual screening approach based on molecular docking, DFT and molecular dynamics simulations studies. 3 Biotech. 2024; 14:83. doi: 10.1007/s13205-023-03912-5.
30- Jung W, Goo S, Hwang T, Lee H, Kim YK, Chae JW, et al. Absorption Distribution Metabolism Excretion and Toxicity Property Prediction Utilizing a Pre-Trained Natural Language Processing Model and Its Applications in Early-Stage Drug Development. Pharmaceuticals (Basel). 2024 Mar 17;17(3):382.
31- Dakal T, Joseph J, Deepika D, Maurya P, Sharma DN, Rajagopal S. Comprehensive report on biochemical, pharmacological, and pharmacokinetic properties of tool compounds relevant to human pathologies. RSC Pharm. 2025;2(3):480-9. doi: 10.1039/D4PM00331D.
32- Wu K, Kwon SH, Zhou X, Fuller C, Wang X, Vadgama J, et al. Overcoming Challenges in Small-Molecule Drug Bioavailability: A Review of Key Factors and Approaches. Int J Mol Sci. 2024 Jan;25(23):13121.
33- Sun, Q. The Hydrophobic Effects: Our Current Understanding. Molecules 2022, 27, 7009. https://doi.org/10.3390/molecules27207009.

AJPS is licensed under a Creative Commons Attribution 4.0 International License